Frequency Dynamics-aware Real-time Marginal Pricing of Electricity

Roohallah Khatami, Abdullah Al-Digs, and Yu Christine Chen
Department of Electrical and Computer Engineering
The University of British Columbia
Vancouver, Canada
{roohallah.khatami, aldigs, chen}@ece.ubc.ca

***Abstract*—This paper presents a frequency dynamics-aware marginal pricing method for real-time electricity markets. The proposed method captures the impact of system frequency dynamics on the marginal price of electricity in the presence of aggressive net-load variations made more likely by greater renewable integration. We formulate a dynamics-aware economic dispatch (ED) by augmenting the traditional single-snapshot ED with constraints pertaining to system frequency dynamics, and frequency deviations from the synchronous speed are penalized in the modified objective function. The resulting ED embeds two distinct time steps to optimize over fast system dynamics and slower decisions on generator set-points. We prove that the dynamics-aware marginal price is the (suitably scaled) Lagrange multiplier of the power balance constraint and that it converges in steady state to the marginal price obtained from traditional ED solved with comparable system load. Numerical case studies involving the Western System Coordinating Council test system validate our findings and confirm added revenue opportunities for generators contributing to frequency regulation.**

***Index Terms*—Economic dispatch, frequency dynamics, frequency regulation, marginal electricity pricing**

I. Introduction

Electricity markets generally embed a multi-stage structure spanning longer scheduling horizons with coarser trading intervals (e.g., day-ahead market) followed by shorter scheduling horizons with finer trading intervals (e.g., real-time market) [1], [2]. The overarching goal of these established practices is to schedule available generation resources so that system operators can maintain the supply-demand balance in real time with lowest cost. Additional market outcomes include prices for energy and ancillary services that provide important incentives to its participants. Standard industry practices were largely designed for a system dominated by high-inertia dispatchable fossil fuel-based generators, which are presently being displaced by low-inertia non-dispatchable renewable energy sources [3]. Despite clear economic and environmental benefits of such a shift, greater share of renewable energy sources in the generation mix poses significant technical challenges for reliable and efficient operations as the system must cope with larger and faster variations in the net-load (system load minus non-dispatchable generation). Critical to enable this shift is to improve existing market designs to accurately compensate generation technologies for the energy they actually produce and thereby foster investments into fast-response inverter-based (dispatchable) sources [4], [5]. These sources may serve to contribute virtual inertia that can be relied upon to quickly offset net-load variations [6].

Fundamental to competitive electricity markets is the concept of marginal pricing that reflects the incremental cost incurred for the system to generate an additional unit of energy. The pertinent pricing problem is commonly known as economic dispatch (ED), which is solved for a single snapshot with the underlying assumption that the system is in steady state. However, establishing markets that accurately reflect the cost of generation in the face of larger and faster variations requires solving operation and pricing problems *prior to* reaching steady state [7]. In this paper, we formulate a multi-time-scale dynamics-aware ED constrained by synchronous generator frequency dynamics, which can be straightforwardly generalized to model inverter-based sources of virtual inertia. The proposed method provides a way to compute dynamics-aware marginal prices for the *energy* needed to regulate system frequency. This is distinct from today's frequency regulation market where generators are paid for reserve *capacity* [1], [2], which may incur greater total operation cost due to growing reserve needs to cope with larger and faster net-load variations.

Prior art to enhance marginal pricing formulations in response to emerging generation technologies include exploring the impact of uncertainty arising from renewable sources [8], [9], inter-temporal ramping constraints [10], and energy storage [11], [12]. Another line of work focuses on pricing and compensating faster dynamics of generation sources [13]–[15]. In [13], power system inertia to ensure frequency stability in worst-case contingencies is procured by designing a Vickrey-Clarke-Groves mechanism, and the cost to procure (real and virtual) inertia is co-optimized with a performance metric that reflects the efficient frequency response. In [14], an enhanced unit commitment (UC) is formulated to jointly optimize the cost of energy and inertia where the maximum permissible rate of change of frequency and frequency nadir dictate the inertia requirement, and the marginal price of providing inertia is obtained from dual variables of pertinent constraints. By proposing a chance-constrained UC with inertia constraints, [15] co-optimizes the energy cost and inertia service while also addressing uncertainty in load. The efforts in [13]–[15] mainly target forward markets and provisionally procure adequate inertia by introducing a new market service. With the review of relevant work established, we next outline our contributions.

Contributions. Unlike prior work in this domain, we directly modify the traditional *dynamics-oblivious ED* into a *dynamics-aware ED* by incorporating generator dynamics as constraints, which can be easily generalized to account for providers of virtual inertia. The proposed multi-time-scale ED embeds the relatively fast system dynamics along with slower decisions on generator set-points in a single optimization problem, while limiting the angular frequency deviations (from synchronous speed) by penalizing them in the objective function. It is worth mentioning that [16] formulates a similar problem except with one time step shared across discretized system dynamics and slower set-points decisions. Also, unlike [16], we focus on marginal pricing and show that the (suitably scaled) Lagrange multiplier of the power balance constraint is the real-time *dynamics-aware marginal price* of electricity, and it embodies the impact of generator dynamics in response to load changes and converges to the marginal price obtained from the traditional dynamics-oblivious ED for a comparable constant load. A detailed state-space model for Lagrange multipliers of the dynamics-aware ED is derived in order to further illustrate the coupling between dynamics-aware marginal price and the system frequency dynamics. Based on the aforementioned analysis, we also provide design considerations for the proposed dynamics-aware ED. Numerical simulations of the proposed marginal pricing approach on the Western System Coordinating Council test system demonstrate broader revenue opportunities for generators to contribute to frequency regulation prior to reaching steady state.

II. Preliminaries

In this section, we introduce the traditional dynamics-oblivious economic dispatch. We also outline pertinent synchronous generator dynamics, from which we construct the power system dynamical model.

A. Traditional Economic Dispatch and Marginal Pricing

Consider a transmission system with G online generators in the set $\mathcal{G} = \{1, \ldots, G\}$ supplying system load (inclusive of losses) $P_\circ^{\mathrm{load}}$. Prevailing ED formulations assume that the power system operates at synchronous steady state. Suppose generator g produces steady-state electrical power $P_{\circ,g}$ with cost function $C_g(P_{\circ,g})$. Then the total cost of generation is $C(P_\circ) = \sum_{g\in\mathcal{G}} C_g(P_{\circ,g})$, where $P_\circ = [P_{\circ,1}, \ldots, P_{\circ,G}]^{\mathrm{T}}$. The traditional ED for a single snapshot is formulated as

$$\underset{P_\circ}{\text{minimize}} \quad C(P_\circ) \tag{1a}$$

$$\text{subject to} \quad \mathbb{1}_G^{\mathrm{T}} P_\circ = P_\circ^{\mathrm{load}}, \quad (\lambda_\circ), \tag{1b}$$

where $\mathbb{1}_G$ is a G-dimensional vector of 1s. The cost function $C(\cdot)$ is assumed to be strictly convex and monotonically increasing for the range of generator outputs we consider. With respect to the problem in (1), the marginal price represents the rate of change of the optimal cost due to variations in $P_\circ^{\mathrm{load}}$. It is equal to the Lagrange multiplier of the power balance constraint, and at the optimal solution,

$$\lambda_\circ^\star \mathbb{1}_G = \frac{\partial C(P_\circ^\star)}{\partial P_\circ^\star}, \tag{2}$$

where the superscript $\star$ denotes the values of the corresponding variables at the optimal solution. Since the ED in (1) assumes steady-state operation, the *dynamics-oblivious* $\lambda_\circ$ does not offer any insights on the price of electricity during transients. This is well aligned with power systems dominated by high-inertia synchronous generators serving slow-varying loads. However, the displacement of fossil fuel-based synchronous generators by low-inertia energy sources is bringing about larger, faster, and more frequent transient excursions away from steady-state operating points. Thus, there is a pressing need to update the ED so that the Lagrange multiplier captures the cost of electricity generation over the transient period. Next, we describe a model for frequency dynamics pertinent to the time scales we consider in this paper.

B. Synchronous Generator Model

For each generator $g \in \mathcal{G}$, let ω_g, P_g^{m}, and P_g denote the electrical angular frequency, turbine mechanical power, and electrical-power output, respectively. Assume each generator initially operates at the steady-state equilibrium point with $\omega_g(0) = \omega_{\mathrm{s}} = 2\pi 60\,\mathrm{rad/s}$, the synchronous speed. Defining $\Delta\omega_g := \omega_g - \omega_{\mathrm{s}}$, pertinent dynamics of generator $g \in \mathcal{G}$ can be described by

$$M_g \Delta\dot{\omega}_g = P_g^{\mathrm{m}} - D_g \Delta\omega_g - P_g, \tag{3}$$

$$\tau_g \dot{P}_g^{\mathrm{m}} = P_g^{\mathrm{r}} - P_g^{\mathrm{m}} - R_g^{-1}\Delta\omega_g, \tag{4}$$

where M_g and D_g denote, respectively, its inertia and damping constants, and τ_g, P_g^{r}, and R_g denote its governor time constant, reference power set-point, and droop constant, respectively [17]. The generator dynamical model in (3)–(4) does not describe dynamics for the generator terminal voltage, automatic voltage regulators, or power system stabilizers. However, we find that the model in (3)–(4) is *sufficiently accurate* to capture the impact of generator-frequency dynamics. Furthermore, although our model does not consider nonlinear effects, e.g., saturation limits, we note that they can be incorporated at the expense of additional notational and computational burden.

Assume that the electrical distances between geographically different parts of the power system are negligible, so that all generator frequencies follow the same transient behaviour, i.e., $\Delta\omega_g = \Delta\omega$ in (3)–(4), $\forall\, g \in \mathcal{G}$ [18]. Also, let $P = [P_1, \ldots, P_G]^{\mathrm{T}}$, $P^{\mathrm{m}} = [P_1^{\mathrm{m}}, \ldots, P_G^{\mathrm{m}}]^{\mathrm{T}}$, and $P^{\mathrm{r}} = [P_1^{\mathrm{r}}, \ldots, P_G^{\mathrm{r}}]^{\mathrm{T}}$. Then system dynamics can be expressed as

$$M \Delta\dot{\omega} = P^{\mathrm{m}} - D\Delta\omega - P, \tag{5}$$

$$\tau \dot{P}^{\mathrm{m}} = P^{\mathrm{r}} - P^{\mathrm{m}} - R^{-1}\mathbb{1}_G \Delta\omega, \tag{6}$$

where $M = [M_1, \ldots, M_G]^{\mathrm{T}}$, $D = [D_1, \ldots, D_G]^{\mathrm{T}}$, $\tau = \mathrm{diag}([\tau_1, \ldots, \tau_G])$, $R^{-1} = \mathrm{diag}([R_1^{-1}, \ldots, R_G^{-1}])$.

III. Marginal Cost of Generation

In this section, we formulate the dynamics-aware marginal pricing problem. We then present its optimality conditions, using which we prove that the Lagrange multiplier attributed to power balance constraint is the marginal price of electricity.

A. Problem Formulation

The dynamics-aware ED aims to optimize the generation schedule generator $g \in \mathcal{G}$ over the scheduling horizon of interest (shorter than 5 minutes), where the generator dynamics are explicitly modelled. This calls for properly accommodating the relatively fast system dynamics, along with the slower decisions on generator reference set-points, into a *single* multi-time-scale optimization problem.

Consider the scheduling horizon of the economic dispatch problem from time t_0 to $t_0 + T$. We introduce two pertinent time steps. The time step corresponding to faster system dynamics is denoted by $\Delta t^{\mathrm{D}} = \frac{T}{N^{\mathrm{D}}}$, which is sufficiently small to model generator dynamics (e.g., $0.05\,[\mathrm{sec}]$). The scheduling horizon then divides into N^{D} intervals collected in the set $\mathcal{T}^{\mathrm{D}}_{t_0} = \{t_0, t_0 + \Delta t^{\mathrm{D}}, \ldots, t_0 + T - \Delta t^{\mathrm{D}}\}$. Next, decisions on generator reference set-points are made over a longer time interval $\Delta t^{\mathrm{S}} = \frac{T}{N^{\mathrm{S}}}$ (e.g., $5\,[\mathrm{sec}]$), which subdivides the scheduling horizon into N^{S} intervals collected in $\mathcal{T}^{\mathrm{S}}_{t_0} = \{t_0, t_0 + \Delta t^{\mathrm{S}}, \ldots, t_0 + T - \Delta t^{\mathrm{S}}\}$. With the above in mind, we formulate the following dynamics-aware ED with fast decisions made every Δt^{D} seconds and slower generator set-points determined every Δt^{S} seconds:

$$\underset{\substack{P^{\mathrm{m}}_t, P_t, P^{\mathrm{r}}_{t'} \\ \Delta\omega_t, \Delta\omega^+_t, \Delta\omega^-_t}}{\text{minimize}} \sum_{t \in \mathcal{T}^{\mathrm{D}}_{t_0}} \left(C(P^{\mathrm{m}}_t) + \kappa(\Delta\omega^+_t + \Delta\omega^-_t) \right) \Delta t^{\mathrm{D}}, \quad \text{(7a)}$$

$$\text{subject to } M\Big(\frac{\Delta\omega_{t+\Delta t^{\mathrm{D}}} - \Delta\omega_t}{\Delta t^{\mathrm{D}}}\Big) = P^{\mathrm{m}}_t - D\Delta\omega_t - P_t, \quad t \in \mathcal{T}^{\mathrm{D}}_{t_0},\ (\alpha_t), \quad \text{(7b)}$$

$$\tau\Big(\frac{P^{\mathrm{m}}_{t+\Delta t^{\mathrm{D}}} - P^{\mathrm{m}}_t}{\Delta t^{\mathrm{D}}}\Big) = P^{\mathrm{r}}_{t'} - P^{\mathrm{m}}_t - R^{-1}\mathbb{1}_G \Delta\omega_t, \quad t \in \mathcal{T}^{\mathrm{D}}_{t_0}, t' \in \mathcal{T}^{\mathrm{S}}_{t_0},\ (\beta_t), \quad \text{(7c)}$$

$$\mathbb{1}^{\mathrm{T}}_G P_t = P^{\mathrm{load}}_t,\ t \in \mathcal{T}^{\mathrm{D}}_{t_0},\ (\lambda_t), \quad \text{(7d)}$$

$$\Delta\omega_t = \Delta\omega^+_t - \Delta\omega^-_t,\ t \in \mathcal{T}^{\mathrm{D}}_{t_0},\ (\zeta_t), \quad \text{(7e)}$$

$$\Delta\omega^+_t, \Delta\omega^-_t \geq 0,\ t \in \mathcal{T}^{\mathrm{D}}_{t_0},\ (\mu^{\omega+}_t, \mu^{\omega-}_t). \quad \text{(7f)}$$

The objective function in (7a) embeds two terms, one for cost of energy and the other reflecting the cost of regulating system frequency. The first term indicates the total operating cost $C(P^{\mathrm{m}}_t) = \sum_{g\in\mathcal{G}} C_g(P^{\mathrm{m}}_{t,g})$, where $C_g(\cdot)$ is the cost function for generator $g \in \mathcal{G}$. The second term penalizes frequency deviations by imposing a penalty factor of $\kappa > 0$ with $\Delta\omega^+_t$ and $\Delta\omega^-_t$ respectively denoting the positive and negative components thereof related through (7e) for $t \in \mathcal{T}^{\mathrm{D}}_{t_0}$. Frequency dynamics are captured by (7b) and (7c), and the system power balance constraint with load P^{load}_t is enforced in (7d). Finally, α_t, β_t, λ_t, ζ_t, $\mu^{\omega+}_t$, and $\mu^{\omega-}_t$ denote the Lagrange multipliers associated with the corresponding equality and inequality constraints in (7b)–(7f), respectively.

Before outlining the optimality conditions of (7), it is worth mentioning that (7) can easily accommodate frequency support from renewable sources by incorporating their operation cost in the objective and virtual synchronous generator dynamics in the constraints. Particularly, the operation cost of renewable sources is typically modelled as zero or a linear function of power output [19], [20], neither of which would change the general structure of (7) when incorporated into the objective. Also, a well-studied way to implement frequency regulation in grid-tied inverters is to modulate the controller reference set-points to mimic a synchronous generator with virtual inertia and damping coefficients [21], [22]. Such a model can be incorporated into (7b) in a straightforward manner.

B. Optimality Conditions

The optimality conditions of (7) are expressed through Karush-Kuhn-Tucker (KKT) conditions. Below, we first formulate the Lagrangian of the dynamics-aware ED in (7), from which KKT conditions are then derived.

1) Lagrangian Function: The Lagrangian of (7) is expressed as follows:

$$\begin{aligned}\mathcal{L} = \sum_{t\in\mathcal{T}^{\mathrm{D}}_{t_0}} \Big(& C(P^{\mathrm{m}}_t) + \kappa(\Delta\omega^+_t + \Delta\omega^-_t)\, \Delta t^{\mathrm{D}} \\ & + \alpha^{\mathrm{T}}_t \Big(P^{\mathrm{m}}_t - D\Delta\omega_t - P_t - M\Big(\frac{\Delta\omega_{t+\Delta t^{\mathrm{D}}} - \Delta\omega_t}{\Delta t^{\mathrm{D}}}\Big)\Big) \\ & + \beta^{\mathrm{T}}_t \Big(P^{\mathrm{r}}_{t'} - P^{\mathrm{m}}_t - R^{-1}\mathbb{1}_G\Delta\omega_t - \tau\Big(\frac{P^{\mathrm{m}}_{t+\Delta t^{\mathrm{D}}} - P^{\mathrm{m}}_t}{\Delta t^{\mathrm{D}}}\Big)\Big) \\ & + \lambda_t(P^{\mathrm{load}}_t - \mathbb{1}_G P_t) + \zeta_t(\Delta\omega^+_t - \Delta\omega^-_t - \Delta\omega_t) \\ & - \mu^{\omega+}_t \Delta\omega^+_t - \mu^{\omega-}_t \Delta\omega^-_t \Big). \end{aligned} \quad (8)$$

2) KKT Conditions: Denote the optimal Lagrangian and the optimal decisions of the problem (7) by, respectively, $\mathcal{L}^\star$ and $\{P^{\mathrm{m}\star}_t, P^\star_t, P^{\mathrm{r}\star}_{t'}, \Delta\omega^\star_t, \Delta\omega^{+\star}_t, \Delta\omega^{-\star}_t\}_{t\in\mathcal{T}^{\mathrm{D}}_{t_0}, t'\in\mathcal{T}^{\mathrm{S}}_{t_0}}$. Also let Lagrange multipliers evaluated at the optimal solution be distinguished with superscript $\star$. As an example, the optimal value of λ_t is represented by $\lambda^\star_t$. The optimal solution respects primal feasibility delineated by (7b)–(7f). It additionally satisfies stationarity conditions, which are expressed as follows:

$$\frac{\partial\mathcal{L}^\star}{\partial\Delta\omega^\star_t} = -\alpha^{\star\mathrm{T}}_t D - \Big(\frac{\alpha^\star_{t-\Delta t^{\mathrm{D}}} - \alpha^\star_t}{\Delta t^{\mathrm{D}}}\Big)^{\mathrm{T}} M - \beta^{\star\mathrm{T}}_t R^{-1}\mathbb{1}_G - \zeta^\star_t = 0, \quad t \in \mathcal{T}^{\mathrm{D}}_{t_0}, \quad (9)$$

$$\frac{\partial\mathcal{L}^\star}{\partial P^{\mathrm{m}\star}_t} = \frac{\partial C(P^{\mathrm{m}\star}_t)}{\partial P^{\mathrm{m}\star}_t}\Delta t^{\mathrm{D}} + \alpha^\star_t - \beta^\star_t - \tau\Big(\frac{\beta^\star_{t-\Delta t^{\mathrm{D}}} - \beta^\star_t}{\Delta t^{\mathrm{D}}}\Big) = \mathbb{0}_G, \quad t \in \mathcal{T}^{\mathrm{D}}_{t_0}, \quad (10)$$

$$\frac{\partial\mathcal{L}^\star}{\partial P^\star_t} = -\alpha^\star_t - \lambda^\star_t\mathbb{1}_G = \mathbb{0}_G, \quad t \in \mathcal{T}^{\mathrm{D}}_{t_0}, \quad (11)$$

$$\frac{\partial\mathcal{L}^\star}{\partial P^{\mathrm{r}\star}_{t'}} = \sum_{t=t'}^{t'+\Delta t^{\mathrm{S}}-\Delta t^{\mathrm{D}}} \beta^\star_t = \mathbb{0}_G, \quad t' \in \mathcal{T}^{\mathrm{S}}_{t_0}, \quad (12)$$

$$\frac{\partial\mathcal{L}^\star}{\partial\Delta\omega^{+\star}_t} = \kappa\Delta t^{\mathrm{D}} + \zeta^\star_t - \mu^{\omega+\star}_t = 0, \quad t \in \mathcal{T}^{\mathrm{D}}_{t_0}, \quad (13)$$

$$\frac{\partial\mathcal{L}^\star}{\partial\Delta\omega^{-\star}_t} = \kappa\Delta t^{\mathrm{D}} - \zeta^\star_t - \mu^{\omega-\star}_t = 0, \quad t \in \mathcal{T}^{\mathrm{D}}_{t_0}. \quad (14)$$

Finally, the optimal solution also satisfies complementary slackness conditions, given by the following:

$$\mu^{\omega-\star}_t \Delta\omega^{-\star}_t = 0, \quad \mu^{\omega+\star}_t \Delta\omega^{+\star}_t = 0, \quad t \in \mathcal{T}^{\mathrm{D}}_{t_0}, \quad (15)$$

$$\mu^{\omega-\star}_t, \mu^{\omega+\star}_t \geq 0, \quad t \in \mathcal{T}^{\mathrm{D}}_{t_0}. \quad (16)$$

The dynamics-aware marginal price represents the rate of change of the system operation cost due to an incremental change in electrical load, while satisfying generator and system static and dynamic constraints. In mathematics terms, the marginal price is expressed as the first derivative of optimal Lagrangian with respect to load. Next we present the first main result of this paper on the dynamics-aware marginal price.

Proposition 1. Given the optimal solution of the problem in (7), $\{P_t^{\mathrm{m}\star}, P_t^\star, P_{t'}^{\mathrm{r}\star}, \Delta\omega_t^\star, \Delta\omega_t^{+\star}, \Delta\omega_t^{-\star}\}_{t\in\mathcal{T}_{t_0}^{\mathrm{D}},\, t'\in\mathcal{T}_{t_0}^{\mathrm{S}}}$, and the optimal Lagrangian $\mathcal{L}^\star$, the dynamics-aware marginal price at time $t \in \mathcal{T}_{t_0}^{\mathrm{D}}$ is calculated as

$$\lambda_t'^\star := \frac{\lambda_t^\star}{\Delta t^{\mathrm{D}}} = \frac{1}{\Delta t^{\mathrm{D}}} \frac{d\mathcal{L}^\star}{dP_t^{\mathrm{load}}}. \tag{17}$$

Proof. Using the chain rule in calculus, we have

$$\begin{aligned} \frac{d\mathcal{L}^\star}{dP_t^{\mathrm{load}}} &= \left(\frac{\partial \mathcal{L}^\star}{\partial P_t^{\mathrm{m}\star}}\right)^{\mathrm{T}} \frac{dP_t^{\mathrm{m}\star}}{dP_t^{\mathrm{load}}} + \left(\frac{\partial \mathcal{L}^\star}{\partial P_t^\star}\right)^{\mathrm{T}} \frac{dP_t^\star}{dP_t^{\mathrm{load}}} \\ &+ \left(\frac{\partial \mathcal{L}^\star}{\partial P_{t'}^{\mathrm{r}\star}}\right)^{\mathrm{T}} \frac{dP_{t'}^{\mathrm{r}\star}}{dP_t^{\mathrm{load}}} + \frac{\partial \mathcal{L}^\star}{\partial \Delta\omega_t^\star} \frac{d\Delta\omega_t^\star}{dP_t^{\mathrm{load}}} + \frac{\partial \mathcal{L}^\star}{\partial \Delta\omega_t^{+\star}} \frac{d\Delta\omega_t^{+\star}}{dP_t^{\mathrm{load}}} \\ &+ \frac{\partial \mathcal{L}^\star}{\partial \Delta\omega_t^{-\star}} \frac{d\Delta\omega_t^{-\star}}{dP_t^{\mathrm{load}}} + \frac{\partial \mathcal{L}^\star}{\partial P_t^{\mathrm{load}}}. \end{aligned} \tag{18}$$

Applying the stationarity conditions (9)–(14), the above simplifies as

$$\frac{d\mathcal{L}^\star}{dP_t^{\mathrm{load}}} = \frac{\partial \mathcal{L}^\star}{\partial P_t^{\mathrm{load}}} = \lambda_t^\star. \tag{19}$$

Finally, division of $\lambda_t^\star$ by Δt^{D} ensures that the marginal price applies for arbitrary Δt^{D} and results in consistent units aligned with the cost function. Particularly, for the cost function with units of $[\$/\mathrm{hr}]$, division by Δt^{D} yields marginal price in units of $[\$/\mathrm{MWh}]$ regardless of the length of Δt^{D}. □

IV. Marginal Price Dynamics

In this section, we explore the properties of the dynamics-aware marginal price by deriving a state-space dynamical system model for the Lagrange multipliers of the equality constraints corresponding to power system dynamics in (7). We further establish the connection between the dynamics-aware marginal price and its dynamics-oblivious counterpart from the traditional ED through steady-state analysis.

A. Dynamical System for Dynamics-aware Marginal Price

The result in Proposition 1 arises from applying the KKT conditions of the optimization problem in (7). Here we use the same set of conditions to derive a dynamical system for the dynamics-aware marginal price.

Proposition 2. Define scaled Lagrange multipliers $\alpha_t'^\star := \alpha_t^\star/\Delta t^{\mathrm{D}}$, $\beta_t'^\star := \beta_t^\star/\Delta t^{\mathrm{D}}$, and $\zeta_t'^\star := \zeta_t^\star/\Delta t^{\mathrm{D}}$. Also let

$$x_t^\star = \begin{bmatrix} \lambda_t'^\star \\ \beta_t'^\star \end{bmatrix}, \quad u_t^\star = \begin{bmatrix} \zeta_t'^\star \\ \frac{\partial C(P_t^{\mathrm{m}\star})}{\partial P_t^{\mathrm{m}\star}} \end{bmatrix}. \tag{20}$$

Further define $M_{\mathrm{eff}} := \mathbb{1}_G^{\mathrm{T}} M$ and $D_{\mathrm{eff}} := \mathbb{1}_G^{\mathrm{T}} D$. Then the optimal trajectory of the dynamics-aware marginal price $\lambda_t'^\star$ is governed by the following discrete-time state-space model:

$$x_t^\star = \frac{1}{\Delta t^{\mathrm{D}}} A_d x_{t-\Delta t^{\mathrm{D}}}^\star + B_d u_t^\star, \tag{21}$$

where

$$A_d = \begin{bmatrix} \frac{M_{\mathrm{eff}}}{k\ell} & \frac{1}{k\ell}\mathbb{1}_G^{\mathrm{T}}(RK)^{-1}\tau \\ -\frac{M_{\mathrm{eff}}}{k} L^{-1}K^{-1}\mathbb{1}_G & -L^{-1}K^{-1}\tau \end{bmatrix}, \tag{22}$$

$$B_d = \begin{bmatrix} -\frac{1}{k\ell} & -\frac{1}{k\ell}\mathbb{1}_G^{\mathrm{T}}(RK)^{-1} \\ \frac{1}{k}L^{-1}K^{-1}\mathbb{1}_G & L^{-1}K^{-1} \end{bmatrix}, \tag{23}$$

with

$$K = I_G - \frac{1}{\Delta t^{\mathrm{D}}}\tau, \quad L = I_G - \frac{1}{k}K^{-1}\mathbb{1}_G\mathbb{1}_G^{\mathrm{T}}R^{-1}, \tag{24}$$

$$k = \frac{M_{\mathrm{eff}}}{\Delta t^{\mathrm{D}}} - D_{\mathrm{eff}}, \quad \ell = 1 - \frac{1}{k}\mathbb{1}_G^{\mathrm{T}}(RK)^{-1}\mathbb{1}_G. \tag{25}$$

We refer interested readers to Appendix A for a proof of Proposition 2. The system inputs are $\zeta_t'^\star$ and $\frac{\partial C(P_t^{\mathrm{m}\star})}{\partial P_t^{\mathrm{m}\star}}$, and they drive dynamics in state variables $\lambda_t'^\star$ and $\beta_t'^\star$. The value of $\zeta_t'^\star$ in (20) is calculated from scaling (13)–(14) by $1/\Delta t^{\mathrm{D}}$ and considering three cases: i) $\Delta\omega_t > 0$, ii) $\Delta\omega_t < 0$, and iii) $\Delta\omega_t = 0$. Specifically, given the complementary slackness conditions in (15)–(16), we have

$$\zeta_t'^\star = \begin{cases} \kappa, & \text{if } \Delta\omega_t < 0, \\ -\kappa, & \text{if } \Delta\omega_t > 0, \\ \frac{\mu_t'^{\omega+\star} - \mu_t'^{\omega-\star}}{2}, & \text{if } \Delta\omega_t = 0, \end{cases} \tag{26}$$

In addition, since the cost of generators is typically approximated as a quadratic function of turbine mechanical powers, the entries in $\frac{\partial C(P_t^{\mathrm{m}\star})}{\partial P_t^{\mathrm{m}\star}}$ would be linear functions of optimal turbine mechanical power at time $t \in \mathcal{T}_{t_0}^{\mathrm{D}}$.

B. Connection to Dynamics-oblivious Marginal Price

Here, we demonstrate that the dynamics-aware marginal price converges, in steady state, to its dynamics-oblivious counterpart obtained by solving the traditional ED in (1). In order to uncover this, we solve the dynamics-aware ED in (7) with a load profile P_t^{load} so that its steady-state value is $P_{\mathrm{ss}}^{\mathrm{load}} = P_\circ^{\mathrm{load}}$, equal to the system load in the dynamics-oblivious ED. We then perform steady-state analysis on (21) by assuming that $x_t^\star = x_{t-\Delta t^{\mathrm{D}}}^\star = x_{\mathrm{ss}}^\star$, i.e., $\lambda_t'^\star = \lambda_{t-\Delta t^{\mathrm{D}}}'^\star = \lambda_{\mathrm{ss}}'^\star$ and $\beta_t'^\star = \beta_{t-\Delta t^{\mathrm{D}}}'^\star = \beta_{\mathrm{ss}}'^\star$.

We first note that for (12) to hold, the steady-state value of $\beta_t^\star$ must be $\beta_{\mathrm{ss}}^\star = 0$. As a result, and by examining (9) and (11) at steady state, we have that $\zeta_{\mathrm{ss}}^\star = \lambda_{\mathrm{ss}}^\star \mathbb{1}_{\mathrm{G}}^{\mathrm{T}} D$. Accordingly, the steady-state value of $\lambda_t'^\star$ satisfies

$$\zeta_{\mathrm{ss}}'^\star = \lambda_{\mathrm{ss}}'^\star \mathbb{1}_{\mathrm{G}}^{\mathrm{T}} D = \lambda_{\mathrm{ss}}'^\star D_{\mathrm{eff}}. \tag{27}$$

Given $\beta_{\mathrm{ss}}^\star = 0$, (21) taken at steady state simplifies as

$$\lambda_{\mathrm{ss}}'^\star = \frac{1}{\Delta t^{\mathrm{D}}} \frac{M_{\mathrm{eff}}}{k\ell} \lambda_{\mathrm{ss}}'^\star - \frac{1}{k\ell}\zeta_{\mathrm{ss}}'^\star - \frac{1}{k\ell}\mathbb{1}_G^{\mathrm{T}}(RK)^{-1}\frac{\partial C(P_{\mathrm{ss}}^{\mathrm{m}\star})}{\partial P_{\mathrm{ss}}^{\mathrm{m}\star}}. \tag{28}$$

By substituting (27) into the above and rearranging the resultant, we get

$$\lambda'^{\star}_{\text{ss}} = \frac{1}{k\ell}\Big(\frac{M_{\text{eff}}}{\Delta t^{\text{D}}} - D_{\text{eff}}\Big)\lambda'^{\star}_{\text{ss}} - \frac{1}{k\ell}\mathbb{1}_G^{\text{T}}(RK)^{-1}\frac{\partial C(P^{\text{m}\star}_{\text{ss}})}{\partial P^{\text{m}\star}_{\text{ss}}},$$
$$\lambda'^{\star}_{\text{ss}} = \frac{1}{\ell}\lambda'^{\star}_{\text{ss}} - \frac{1}{k\ell}\mathbb{1}_G^{\text{T}}(RK)^{-1}\frac{\partial C(P^{\text{m}\star}_{\text{ss}})}{\partial P^{\text{m}\star}_{\text{ss}}},$$
$$\ell\lambda'^{\star}_{\text{ss}} = \lambda'^{\star}_{\text{ss}} - \frac{1}{k}\mathbb{1}_G^{\text{T}}(RK)^{-1}\frac{\partial C(P^{\text{m}\star}_{\text{ss}})}{\partial P^{\text{m}\star}_{\text{ss}}}, \tag{29}$$

where the second equality above is obtained by recognizing that $k = \frac{M_{\text{eff}}}{\Delta t^{\text{D}}} - D_{\text{eff}}$ (as defined in (25)). Further rearranging (29) while considering that $\ell - 1 = -\frac{1}{k}\mathbb{1}_G^{\text{T}}(RK)^{-1}\mathbb{1}_G$ (as defined in (25)), the resultant simplifies as

$$\lambda'^{\star}_{\text{ss}}\mathbb{1}_G = \frac{\partial C(P^{\text{m}\star}_{\text{ss}})}{\partial P^{\text{m}\star}_{\text{ss}}}. \tag{30}$$

Next we show that $P^{\text{m}\star}_{\text{ss}} = P^{\star}_{\circ}$, from which $\lambda'^{\star}_{\text{ss}} = \lambda^{\star}_{\circ}$ follows. Let the optimal trajectory of the physical system reach the steady state, with $\Delta\omega^{\star}_{t+\Delta t^{\text{D}}} = \Delta\omega^{\star}_{t} = \Delta\omega^{\star}_{\text{ss}}$ and $P^{\text{m}\star}_{t+\Delta t^{\text{D}}} = P^{\text{m}\star}_{t} = P^{\text{m}\star}_{\text{ss}}$ in (7b) and (7c) so they become

$$\mathbb{0}_G = P^{\text{m}\star}_{\text{ss}} - D\Delta\omega^{\star}_{\text{ss}} - P^{\star}_{\text{ss}}. \tag{31}$$
$$\mathbb{0}_G = P^{\text{r}\star}_{\text{ss}} - P^{\text{m}\star}_{\text{ss}} - R^{-1}\mathbb{1}_G\Delta\omega^{\star}_{\text{ss}}. \tag{32}$$

Now, for a setting comparable to that of (1) solved at synchronous steady state, we set $\Delta\omega^{\star}_{\text{ss}} = 0$.[1] Then we get from (31) that the generator output power converges to $P^{\star}_{\text{ss}} = P^{\text{m}\star}_{\text{ss}}$ in steady state. We can then rewrite (30) and solve the following system of equations to obtain the optimal solution at steady state:

$$\lambda'^{\star}_{\text{ss}}\mathbb{1}_G = \frac{\partial C(P^{\star}_{\text{ss}})}{\partial P^{\star}_{\text{ss}}}, \tag{33}$$
$$\mathbb{1}_G^{\text{T}}P^{\star}_{\text{ss}} = P^{\text{load}}_{\text{ss}} = P^{\text{load}}_{\circ}, \tag{34}$$

where (34) is the power balance in (7d) evaluated at steady state. Note that (33)–(34) represent the same set of algebraic equations as the combination of (2) and (1b), which can be solved to yield the exact same solution, i.e., $\lambda^{\star}_{\circ} = \lambda'^{\star}_{\text{ss}}$ and $P^{\star}_{\circ} = P^{\star}_{\text{ss}}$. We conclude that the dynamics-aware price and generator outputs indeed converge to their counterparts solved from the dynamics-oblivious ED.

C. Design Considerations in Dynamics-aware ED

Via the proposition below, we outline suitable choice of κ in (7a) to ensure steady-state frequency deviation $\Delta\omega^{\star}_{\text{ss}} = 0$.

Proposition 3. Suppose the system load undergoes an increase from an initial value of $P^{\text{load}}_{t_0}$ to reach a new steady-state load of $P^{\text{load}}_{\text{ss}}$ at the end of the scheduling horizon. Then the steady-state frequency deviation $\Delta\omega^{\star}_{\text{ss}} = 0$ if and only if

$$\kappa \geq \lambda^{\star}_{\circ}D_{\text{eff}}, \tag{35}$$

where $\lambda^{\star}_{\circ}$ is the marginal price solved from the traditional dynamics-oblivious ED for the load $P^{\text{load}}_{\circ} = P^{\text{load}}_{\text{ss}}$.

[1] In Section IV-C, we show that $\Delta\omega^{\star}_{\text{ss}} = 0$ indeed holds if κ in the objective function of (7) satisfies a particular condition.

Proof. Consider the post-disturbance steady state, and let the subscript ss denote the value the corresponding variable takes at steady state. We first sum (31) over all $g \in \mathcal{G}$ to get

$$\mathbb{1}_G^{\text{T}}P^{\text{m}\star}_{\text{ss}} - D_{\text{eff}}\Delta\omega^{\star}_{\text{ss}} = P^{\text{load}}_{\circ}. \tag{36}$$

Next, rearranging (27) and scaling the resultant by $\mathbb{1}_G$, we get

$$\lambda'^{\star}_{\text{ss}}\mathbb{1}_G = \frac{\zeta'^{\star}_{\text{ss}}}{D_{\text{eff}}}\mathbb{1}_G = \left(\frac{\kappa - \mu'^{\omega-\star}_{\text{ss}}}{D_{\text{eff}}}\right)\mathbb{1}_G, \tag{37}$$

where the second equality is obtained by substituting (14) scaled by $1/\Delta t^{\text{D}}$ and defining $\mu'^{\omega-\star}_{\text{ss}} := \mu^{\omega-\star}_{\text{ss}}/\Delta t^{\text{D}}$.

Suppose (35) holds, we examine (36)–(37) for two cases.

(i) $\kappa = \lambda^{\star}_{\circ}D_{\text{eff}}$: Substitution of κ into (37) yields

$$\lambda'^{\star}_{\text{ss}}\mathbb{1}_G = \left(\lambda^{\star}_{\circ} - \frac{\mu'^{\omega-\star}_{\text{ss}}}{D_{\text{eff}}}\right)\mathbb{1}_G. \tag{38}$$

Further substitute (2) and (30) into the above to get

$$\frac{\partial C(P^{\text{m}\star}_{\text{ss}})}{\partial P^{\text{m}\star}_{\text{ss}}} = \frac{\partial C(P^{\star}_{\circ})}{\partial P^{\star}_{\circ}} - \frac{\mu'^{\omega-\star}_{\text{ss}}}{D_{\text{eff}}}\mathbb{1}_G. \tag{39}$$

Suppose $\mu'^{\omega-\star}_{\text{ss}} > 0$ implying $\frac{\partial C(P^{\text{m}\star}_{\text{ss}})}{\partial P^{\text{m}\star}_{\text{ss}}} < \frac{\partial C(P^{\star}_{\circ})}{\partial P^{\star}_{\circ}}$. Since $C(\cdot)$ is strictly convex, its partial derivative is an increasing function, and so $P^{\text{m}\star}_{\text{ss}} < P^{\star}_{\circ}$ and $\mathbb{1}_G^{\text{T}}P^{\text{m}\star}_{\text{ss}} < \mathbb{1}_G^{\text{T}}P^{\star}_{\circ}$. With this in mind, a comparison of (1b) and (36) yields the conclusion that $\Delta\omega^{\star}_{\text{ss}} < 0$, and from complementary slackness condition (15) we get $\mu'^{\omega-\star}_{\text{ss}} = 0$, a contradiction to the assumption that $\mu'^{\omega-\star}_{\text{ss}} > 0$. Thus, it must be the case that $\mu'^{\omega-\star}_{\text{ss}} = 0$, which implies that $\frac{\partial C(P^{\star}_{\circ})}{\partial P^{\star}_{\circ}} = \frac{\partial C(P^{\text{m}\star}_{\text{ss}})}{\partial P^{\text{m}\star}_{\text{ss}}}$ by (39). Since $C(\cdot)$ is a monotonically increasing function in the region of interest, the above implies that $\mathbb{1}_G^{\text{T}}P^{\text{m}\star}_{\text{ss}} = \mathbb{1}_G^{\text{T}}P^{\star}_{\circ}$, requiring $\Delta\omega^{\star}_{\text{ss}} = 0$ for both (1b) and (36) to hold.

(ii) $\kappa > \lambda^{\star}_{\circ}D_{\text{eff}}$: Substituting κ into (37) while considering (2) and (30) yields

$$\frac{\partial C(P^{\text{m}\star}_{\text{ss}})}{\partial P^{\text{m}\star}_{\text{ss}}} > \frac{\partial C(P^{\star}_{\circ})}{\partial P^{\star}_{\circ}} - \frac{\mu'^{\omega-\star}_{\text{ss}}}{D_{\text{eff}}}\mathbb{1}_G. \tag{40}$$

Suppose $\mu'^{\omega-\star}_{\text{ss}} = 0$ implying $\frac{\partial C(P^{\text{m}\star}_{\text{ss}})}{\partial P^{\text{m}\star}_{\text{ss}}} > \frac{\partial C(P^{\star}_{\circ})}{\partial P^{\star}_{\circ}}$. Since $C(\cdot)$ is strictly convex, we have that $\mathbb{1}_G^{\text{T}}P^{\text{m}\star}_{\text{ss}} > \mathbb{1}_G^{\text{T}}P^{\star}_{\circ}$, which then implies that $\Delta\omega^{\star}_{\text{ss}} > 0$ for both (1b) and (36) to hold. However, for any $\Delta\omega^{\star}_{\text{ss}} > 0$, there exists $\epsilon > 0$ such that $\Delta\widetilde{\omega}^{\star}_{\text{ss}} := \Delta\omega^{\star}_{\text{ss}} - \epsilon$ leads to lower cost. Specifically, in (7a), the penalty term pertinent to frequency deviation is reduced, *and* the term pertinent to generation is reduced because less turbine mechanical power is needed to meet the load according to (36). Thus $\Delta\omega^{\star}_{\text{ss}} > 0$ would, in fact, *not* be the optimal solution, a contradiction. Thus, $\mu'^{\omega-\star}_{\text{ss}} > 0$, from which $\Delta\omega^{\star}_{\text{ss}} = 0$ follows by the complementary slackness condition in (15).

Combining the above, we see that setting $\kappa \geq \lambda^{\star}_{\circ}D_{\text{eff}}$ indeed ensures $\Delta\omega^{\star}_{\text{ss}} = 0$.

Next, consider the other direction, which is equivalent to showing $\kappa < \lambda^{\star}_{\circ}D_{\text{eff}}$ implies $\Delta\omega^{\star}_{\text{ss}} \neq 0$. Substitution of $\kappa < \lambda^{\star}_{\circ}D_{\text{eff}}$ into (37) yields

$$\lambda'^{\star}_{\text{ss}}\mathbb{1}_G < \left(\lambda^{\star}_{\circ} - \frac{\mu'^{\omega-\star}_{\text{ss}}}{D_{\text{eff}}}\right)\mathbb{1}_G. \tag{41}$$

With (2) and (30) in mind, the above leads to

$$\frac{\partial C(P_{\mathrm{ss}}^{\mathrm{m}\star})}{\partial P_{\mathrm{ss}}^{\mathrm{m}\star}} < \frac{\partial C(P_{\circ}^{\star})}{\partial P_{\circ}^{\star}} - \frac{\mu_{\mathrm{ss}}^{\prime\omega-\star}}{D_{\mathrm{eff}}}\mathbb{1}_G \leq \frac{\partial C(P_{\circ}^{\star})}{\partial P_{\circ}^{\star}}, \tag{42}$$

where we have used the complementary slackness condition that $\mu_{\mathrm{ss}}^{\prime\omega-\star} \geq 0$. Since $C(P_{\mathrm{ss}}^{\mathrm{m}\star})$ is convex, its partial derivative is an increasing function, and so $\mathbb{1}_G^{\mathrm{T}} P_{\mathrm{ss}}^{\mathrm{m}\star} < \mathbb{1}_G^{\mathrm{T}} P_{\circ}^{\star}$. Finally, comparison between (1b) and (36) shows that $\Delta\omega_{\mathrm{ss}}^{\star} < 0$. Thus, $\Delta\omega_{\mathrm{ss}}^{\star} \neq 0$, which concludes the proof. □

Beyond the rigorous proof for Proposition 3 above, we next offer an intuitive yet insightful argument to support it.

Remark 1 (Intuition Behind Proposition 3)**.** We observe from (36) that the new load is balanced through a combination of generation and frequency deviation scaled by the sum of damping constants. If the frequency deviation were not penalized, the term $-D_{\mathrm{eff}}\Delta\omega_{\mathrm{ss}}^{\star} =: P_{\mathrm{ss}}^{\omega\star}$ would essentially represent a virtual and indeed "free" source of energy. In this case, the optimization problem would leverage the virtual source through suitable adjustment of $P_{\mathrm{ss}}^{\mathrm{r}\star}$ in (32) rendering $\Delta\omega_{\mathrm{ss}}^{\star}$ nonzero. In our problem formulation, the frequency deviation penalization term in (7a) may be interpreted as a "virtual" market participant bidding the amount $P_{\mathrm{ss}}^{\omega\star}$ with cost

$$C^{\omega}(P_{\mathrm{ss}}^{\omega\star}) = \frac{\kappa}{D_{\mathrm{eff}}} P_{\mathrm{ss}}^{\omega\star}, \tag{43}$$

at the optimal steady-state solution. Based on the argument above, for sufficiently large κ, the use of $P_{\mathrm{ss}}^{\omega\star}$ would no longer be economically justifiable, leading to $\Delta\omega_{\mathrm{ss}}^{\star} = 0$. □

Remark 2 (Consistency with Traditional ED)**.** Consistency with the traditional ED requires the system frequency and marginal price trajectories from the solution of the dynamics-aware ED converge to their dynamics-oblivious counterparts solved with a comparable constant load. To this end, the dynamics-aware marginal pricing problem ought to: i) regulate system frequency via a penalty term in the objective function (as in our problem formulation in (7)) *or* a controller (e.g., automatic generation control) embedded in the constraints, and ii) designate generator set-points as decision variables rather than predetermined inputs. The necessity of condition i) is established through Proposition 3 as lack of frequency regulation implies $\kappa = 0$ in the objective function, thus violating (35). The optimizer then gives rise to nonzero steady-state frequency deviation, which is inconsistent with traditional ED. To demonstrate the necessity of condition ii), let us suppose that $P_{t'}^{\mathrm{r}\star}$, $t' \in \mathcal{T}_{t_0}^{\mathrm{S}}$, are preset generator set-points obtained from the solution of the dynamics-oblivious ED in (1), so that they are no longer decision variables in the dynamics-aware ED. Although the optimal solution of such a hypothetical pricing problem leads to zero steady-state frequency deviation with $P_{t'}^{\mathrm{r}\star}$ obtained from the traditional ED, the resulting marginal price trajectory is substantially different from the optimal solution of (7). Examining the optimality conditions of the hypothetical problem in steady state reveals that the absence of (12) (as generator set-points are no longer decision variables) would allow $\beta_{\mathrm{ss}}^{\prime\star}$ to take a positive value. Then,

TABLE I: Dynamic Model Parameters of Generators and Governors

Generator	M_g [sec]	D_g	τ_g [sec]	$\frac{1}{R_g}$
$g = 1$	23.64	20	2	100
$g = 2$	6.4	20	2	100
$g = 3$	3.01	20	2	100

TABLE II: Generator Quadratic Cost Function Parameters

Generator	a_g [\$/(MW^{2}h)]	b_g [\$/MWh]	c_g [\$/h]
$g = 1$	0.1100	5	0
$g = 2$	0.0850	1.2	0
$g = 3$	0.1225	1	0

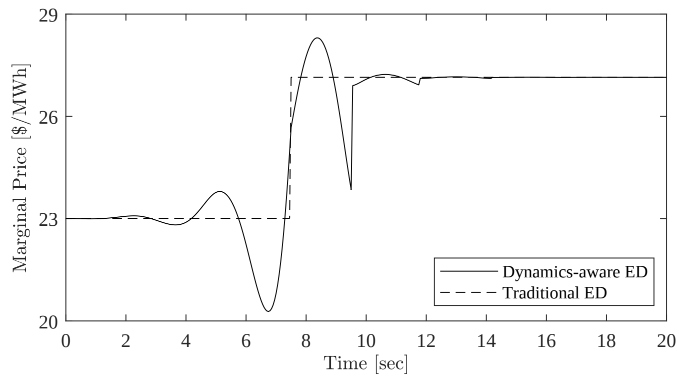

Fig. 1: Marginal prices from dynamics-aware and traditional EDs.

from (10), we get $\lambda_{\mathrm{ss}}^{\prime\star} = \frac{\partial C(P_{\mathrm{ss}}^{\mathrm{m}\star})}{\partial P_{\mathrm{ss}}^{\mathrm{m}\star}} - \beta_{\mathrm{ss}}^{\prime\star}$. Since the optimal solution of the hypothetical problem in steady state coincides with that of traditional ED, then $\frac{\partial C(P_{\mathrm{ss}}^{\mathrm{m}\star})}{\partial P_{\mathrm{ss}}^{\mathrm{m}\star}} = \frac{\partial C(P_{\circ}^{\star})}{\partial P_{\circ}^{\star}} = \lambda_{\circ}^{\star}$ leading to $\lambda_{\mathrm{ss}}^{\prime\star} = \lambda_{\circ}^{\star} - \beta_{\mathrm{ss}}^{\prime\star} < \lambda_{\circ}^{\star}$, a patent inconsistency. □

V. Numerical Results

Three generators are used for the simulations, and their dynamic model and cost function parameters are respectively provided in Tables I and II. The generator parameters are adopted from the Western System Coordinating Council (WSCC) with the system power base being 100 [MVA] [23]. The scheduling horizon covers 20 [sec] from $t_0 = 0$ [sec] to $t_0 + T = 20$ [sec]. The faster time step capturing system dynamics is $\Delta t^{\mathrm{D}} = 0.05$ [sec], while the generator set-point decisions are made every $\Delta t^{\mathrm{S}} = 2.5$ [sec]. The system load takes a constant value of 300 [MW] for $t \in [0, 7.5]$ [sec], followed by a 20% increase for $t \in (7.5, 20]$ [sec]. Also, the penalty factor κ is set to be slightly greater than the value on the right-hand side of (35).

A. Benchmark Dynamic and Steady-state Comparisons

Here we present the simulation results for the optimal solution of the dynamics-aware ED in (7), and comparisons are made with respect to the solution of the traditional ED in (1). Both versions of the ED are implemented in GAMS and solved using the CPLEX 12.6.2 package [24]. Note that we solve the traditional ED twice, the first with the initial load and the second with the post-disturbance steady-state load, thus leading to two different marginal prices.

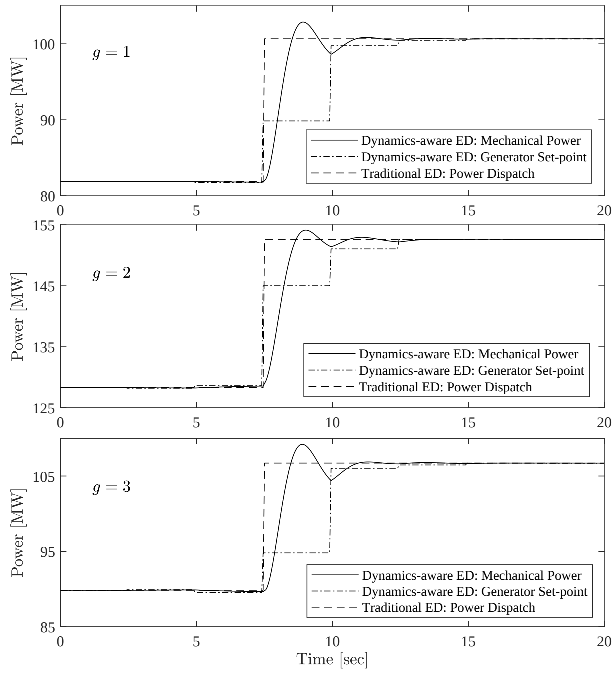

Fig. 2: Traditional and dynamics-aware ED power schedule for (a) generator 1, (b) generator 2, (c) generator 3.

1) Marginal Price: The marginal prices resulting from the traditional and dynamics-aware EDs are plotted in Fig. 1. Indeed, as shown in Section IV-B, the dynamics-aware marginal price converges in steady state to the same value of the dynamics-oblivious counterpart corresponding to the new load. We also verify that the marginal price trajectory obtained from simulating the discrete-time dynamical system in (21) with the optimal decisions $P_t^{\mathrm{m}\star}$ and $\zeta_t^{\prime\star}$ as the input vector $u_t^{\star}$ exactly matches that from CPLEX depicted as the solid trace in Fig. 1.

2) Generator Power: The power dispatch of generators for traditional ED, as well as the generator set-points and the associated mechanical power for dynamics-aware ED, are plotted in Fig. 2 for $g \in \{1, 2, 3\}$. As expected, trajectories from the dynamics-aware ED converge in steady state to the set-points obtained from solving the traditional ED with the new load. Unlike the traditional ED that approximates mechanical power of generators by step-wise functions, the dynamics-aware ED more accurately models the mechanical power, governed by updated set-points, and delineates its sub-interval variations. Thus, the aggregated mechanical power from generators follow the system load closely while co-optimizing the operation cost and frequency deviations. In addition, since the decisions on generator set-points are made based on load changes throughout the entire scheduling horizon, the dynamic-aware ED solution preemptively adjusts the generator set-points even before the load changes at time $t = 10\,[\mathrm{sec}]$, alleviating the ensuing frequency deviations.

3) Frequency Deviation: As shown in Fig. 3a, due to the increase in load, the system frequency decreases (negative $\Delta\omega_t$) starting at time $t = 7.5\,[\mathrm{sec}]$. Proper choice of the penalty factor κ leads to recovery of the system frequency within $5\,[\mathrm{sec}]$. Also, by preemptively adjusting the generator

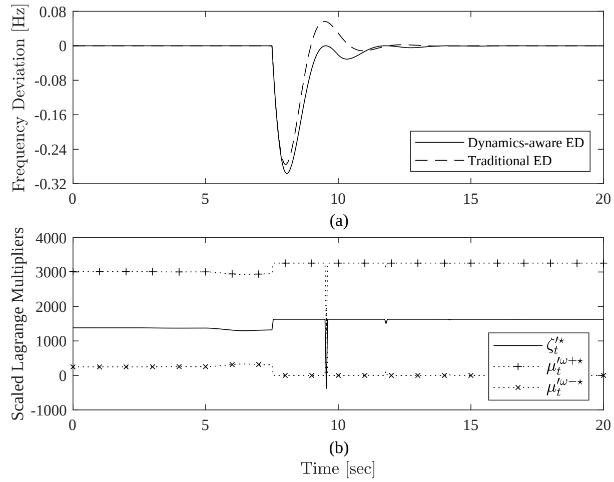

Fig. 3: Time-domain trajectories for (a) system frequency deviations and (b) scaled Lagrange multipliers.

set-points, the solution of the dynamics-aware ED leads to lower transient frequency deviations compared to that of the dynamics-oblivious ED. In Fig 3b, we plot the scaled Lagrange multipliers of equality and inequality constraints pertaining to frequency (i.e., $\zeta_t^{\prime\star}$, $\mu_t^{\prime\omega+\star}$, and $\mu_t^{\prime\omega-\star}$). We also verify through Fig. 3 that $\zeta_t^{\prime\star} = \kappa$ for $\Delta\omega_t < 0$ and $\zeta_t^{\prime\star} = \frac{\mu_t^{\prime\omega+\star} - \mu_t^{\prime\omega-\star}}{2}$ for $\Delta\omega_t = 0$, consistent with (26).

B. Revenues, Costs, and Profits

In this case study, we compare the revenues and profits for generators realized by using the marginal prices resulting from the traditional ED and the proposed dynamics-aware ED. In industry-standard real-time electricity markets [1], the traditional ED is typically run every $5\,[\mathrm{min}]$, so the corresponding dynamics-oblivious marginal price does not reflect the impact of load variations within the look-ahead interval. As an example, consider the load profile used in Section V-A. Despite the 20% load increase at $t = 7.5\,[\mathrm{sec}]$, the generators would in fact be compensated at a constant marginal price for the entire 5-minute scheduling horizon based on the initial load of $300\,[\mathrm{MW}]$. The dynamics-aware ED, however, discerns the load change and captures its impact on the marginal price as shown in Fig. 1. Thus, the dynamics-aware marginal price recovers profits that might have been otherwise missed using dynamics-oblivious marginal price.

To examine the proposed pricing practice against the traditional counterpart, we consider load increases of 5%, 10%, 15%, and 20%, each imposed at time $t = 7.5\,[\mathrm{sec}]$. The total generation cost is calculated as

$$\sum_{t \in \mathcal{T}_{t_0}^{\mathrm{D}}} C(P_t^{\mathrm{m}\star}) \Delta t^{\mathrm{D}}, \tag{44}$$

and the revenue is calculated as

$$\sum_{t \in \mathcal{T}_{t_0}^{\mathrm{D}}} \lambda_t^{\prime\star} \mathbb{1}_G^{\mathrm{T}} P_t^{\mathrm{m}\star} \Delta t^{\mathrm{D}}, \tag{45}$$

for both versions of ED. Total profit is then obtained by subtracting cost from revenue. In the proposed dynamics-aware

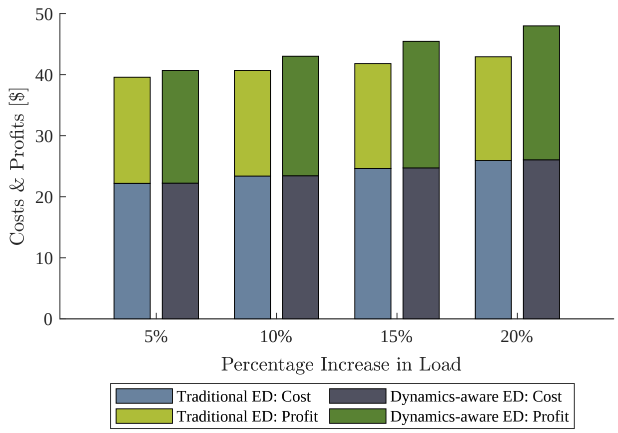

Fig. 4: Aggregate costs and profits of generators from traditional and dynamics-aware ED for different percentage increases in load.

ED, the generator mechanical power $P_t^{\mathrm{m}\star}$ and dynamics-aware marginal price $\lambda_t'^\star$ are readily available from the solution of optimization problem (7). For comparison, we solve the traditional ED for the initial load to obtain the optimal generator set-points and the corresponding dynamics-oblivious marginal price $\lambda_\circ^\star$. To extract the mechanical power trajectories, we apply the optimal set-points from the traditional ED solution as the generator references in a dynamic simulation performed in PSAT [25], where the system frequency is regulated with an industry-standard AGC (see, e.g., [26] for model details). Also, to calculate the revenue in the dynamics-oblivious case, we set $\lambda_t'^\star = \lambda_\circ^\star$, $\forall\, t \in \mathcal{T}_{t_0}^{\mathrm{D}}$, in (45). In Fig. 4, for each load change scenario, we plot the total cost and profit, which sum to the total revenue. Visual examination of Fig. 4 reveals that the dynamics-aware marginal pricing yields greater revenues and profits for generators compared to the traditional dynamics-oblivious counterpart, while the two methods lead to nearly identical generation costs.

C. Computation Time

The proposed dynamics-aware ED is modelled in GAMS and solved using the CPLEX solver, on a desktop computer with a 2.7 [GHz] i7 processor and 16 [GB] of RAM. The simulation time for the 3-generator WSCC test system is 0.39 [sec]. Furthermore, in order to examine the scalability of the proposed dynamics-aware ED, we also simulate the 10-generator New England test system [27], resulting in a computation time of 2.47 [sec].

VI. Concluding Remarks and Directions for Future Work

In this paper, we presented a dynamics-aware marginal pricing scheme that incorporates power system dynamics as constraints and penalizes frequency deviations from the synchronous speed in the objective function. The dynamics-aware marginal price, that is proven to be the (suitably scaled) Lagrange multiplier of dynamics-aware ED, reflects the system dynamics after load disturbances and converges to the solution of the traditional ED in steady state. Our analysis is supported rigorous mathematical proofs, from which conclusive arguments are made toward design considerations in the dynamics-aware ED. Numerical results validate the analytical derivations and confirm the benefits of the proposed dynamics-aware marginal price in providing broader revenue opportunities for generators prior to reaching steady state. Future work includes investigating the impact of other frequency regulation schemes on the dynamics-aware marginal price, extension to dynamics-aware *locational* marginal pricing of electricity, and addressing forecast uncertainties through coordinated dynamics- and risk-aware marginal pricing of energy and reserve capacity. Also of importance are improvements in computation time by increasing the discretization time step and exploring other optimization solver algorithms.

Appendix

A. Proof of Proposition 2

Stationarity conditions in (9)–(11) can be equivalently expressed using the scaled Lagrange multipliers

$$0 = -\alpha_t'^{\star\mathrm{T}} D - \left(\frac{\alpha'^{\star}_{t-\Delta t^{\mathrm{D}}} - \alpha_t'^{\star}}{\Delta t^{\mathrm{D}}}\right)^{\mathrm{T}} M - \beta_t'^{\star\mathrm{T}} R^{-1}\mathbb{1}_G - \zeta_t'^{\star}, \quad t \in \mathcal{T}_{t_0}^{\mathrm{D}}, \tag{46}$$

$$\mathbb{0}_G = \frac{\partial C(P_t^{\mathrm{m}\star})}{\partial P_t^{\mathrm{m}\star}} + \alpha_t'^{\star} - \beta_t'^{\star} - \tau\left(\frac{\beta'^{\star}_{t-\Delta t^{\mathrm{D}}} - \beta_t'^{\star}}{\Delta t^{\mathrm{D}}}\right), \quad t \in \mathcal{T}_{t_0}^{\mathrm{D}}, \tag{47}$$

$$\mathbb{0}_G = -\alpha_t'^{\star} - \lambda_t'^{\star}\mathbb{1}_G, \quad t \in \mathcal{T}_{t_0}^{\mathrm{D}}, \tag{48}$$

Then rearrange (48) and substitute the resultant into (46) and (47) to get, respectively,

$$0 = \lambda_t'^{\star} D_{\mathrm{eff}} + \frac{\lambda'^{\star}_{t-\Delta t^{\mathrm{D}}} - \lambda_t'^{\star}}{\Delta t^{\mathrm{D}}} M_{\mathrm{eff}} - \beta_t'^{\star\mathrm{T}} R^{-1}\mathbb{1}_G - \zeta_t'^{\star}, \tag{49}$$

$$\mathbb{0}_G = \frac{\partial C(P_t^{\mathrm{m}\star})}{\partial P_t^{\mathrm{m}\star}} - \lambda_t'^{\star}\mathbb{1}_G - \beta_t'^{\star} - \tau\left(\frac{\beta'^{\star}_{t-\Delta t^{\mathrm{D}}} - \beta_t'^{\star}}{\Delta t^{\mathrm{D}}}\right), \tag{50}$$

for all $t \in \mathcal{T}_{t_0}^{\mathrm{D}}$. Further rearrange (49)–(50) to get

$$\lambda_t'^{\star} = \frac{1}{k}\left(\frac{M_{\mathrm{eff}}}{\Delta t^{\mathrm{D}}}\lambda'^{\star}_{t-\Delta t^{\mathrm{D}}} - \mathbb{1}_G^{\mathrm{T}} R^{-1}\beta_t'^{\star} - \zeta_t'^{\star}\right), \tag{51}$$

$$\beta_t'^{\star} = K^{-1}\left(\frac{\partial C(P_t^{\mathrm{m}\star})}{\partial P_t^{\mathrm{m}\star}} - \mathbb{1}_G\lambda_t'^{\star} - \frac{1}{\Delta t^{\mathrm{D}}}\tau\beta'^{\star}_{t-\Delta t^{\mathrm{D}}}\right). \tag{52}$$

The system of $G+1$ difference equations above describes the discrete-time dynamics of the scaled Lagrange multipliers. Substitution of (52) into (51) (and vice-versa) followed by straightforward algebraic manipulation yields the state-space model in (21).

References

[1] "Business practice manual for market operations, version 65," California ISO, 2020.

[2] "Business practices manual: Energy and operating reserve markets," Midcontinent ISO, 2016.

[3] E. Ela, V. Diakov, E. Ibanez, and M. Heaney, "Impacts of variability and uncertainty in solar photovoltaic generation at multiple timescales," National Renewable Energy Laboratory (NREL), Golden, CO, United States, Tech. Rep., 2013.

[4] Australian Energy Market Commission, "System security market frameworks review, final report," Tech. Rep., June 2017.

[5] E. Ela, C. Wang, S. Moorty, K. Ragsdale, J. O'Sullivan, M. Rothleder, and B. Hobbs, "Electricity markets and renewables: a survey of potential design changes and their consequences," *IEEE Power and Energy Magazine*, vol. 15, no. 6, pp. 70–82, Oct. 2017.

[6] P. Denholm, T. Mai, R. W. Kenyon, B. Kroposki, and M. O'malley, "Inertia and the power grid: A guide without the spin," National Renewable Energy Laboratory, Tech. Rep., 2020. [Online]. Available: https://www.nrel.gov/docs/fy20osti/73856.pdf

[7] N. Li, C. Zhao, and L. Chen, "Connecting automatic generation control and economic dispatch from an optimization view," *IEEE Transactions on Control of Network Systems*, vol. 3, no. 3, pp. 254–264, Jul. 2015.

[8] X. Fang, B.-M. Hodge, E. Du, C. Kang, and F. Li, "Introducing uncertainty components in locational marginal prices for pricing wind power and load uncertainties," *IEEE Transactions on Power Systems*, vol. 34, no. 3, pp. 2013–2024, Jan. 2019.

[9] X. Fang, H. Cui, E. Du, F. Li, and C. Kang, "Characteristics of locational uncertainty marginal price for correlated uncertainties of variable renewable generation and demands," *Applied Energy*, vol. 282, p. 116064, Jan. 2021.

[10] J. Zhao, T. Zheng, and E. Litvinov, "A multi-period market design for markets with intertemporal constraints," *IEEE Transactions on Power Systems*, vol. 35, no. 4, pp. 3015–3025, Dec. 2019.

[11] J. A. Taylor, "Financial storage rights," *IEEE Transactions on Power Systems*, vol. 30, no. 2, pp. 997–1005, 2014.

[12] R. Khatami and M. Parvania, "Spatio-temporal value of energy storage in transmission networks," *IEEE Systems Journal*, vol. 14, no. 3, pp. 3855–3864, Jan. 2020.

[13] B. K. Poolla, S. Bolognani, N. Li, and F. Dörfler, "A market mechanism for virtual inertia," *IEEE Transactions on Smart Grid*, vol. 11, no. 4, pp. 3570–3579, Jan. 2020.

[14] L. Badesa, F. Teng, and G. Strbac, "Pricing inertia and frequency response with diverse dynamics in a mixed-integer second-order cone programming formulation," *Applied Energy*, vol. 260, p. 114334, 2020.

[15] Z. Liang, R. Mieth, and Y. Dvorkin, "Inertia pricing in stochastic electricity markets," 2021. [Online]. Available: https://arxiv.org/abs/2107.04101v1

[16] G. Zhang, J. McCalley, and Q. Wang, "An agc dynamics-constrained economic dispatch model," *IEEE Transactions on Power Systems*, vol. 34, no. 5, pp. 3931–3940, 2019.

[17] P. W. Sauer and M. A. Pai, *Power System Dynamics and Stability*. Upper Saddle River, NJ: Prentice-Hall, Inc., 1998.

[18] M. D. Ilić and Q. Liu, *Toward Sensing, Communications and Control Architectures for Frequency Regulation in Systems with Highly Variable Resources*. New York, NY: Springer New York, 2012, pp. 3–33.

[19] F. Bouffard and F. D. Galiana, "Stochastic security for operations planning with significant wind power generation," in *2008 IEEE Power and Energy Society General Meeting-Conversion and Delivery of Electrical Energy in the 21st Century*. IEEE, 2008, pp. 1–11.

[20] N. Augustine, S. Suresh, P. Moghe, and K. Sheikh, "Economic dispatch for a microgrid considering renewable energy cost functions," in *2012 IEEE PES Innovative Smart Grid Technologies (ISGT)*. IEEE, 2012, pp. 1–7.

[21] S. Dong and Y. C. Chen, "Adjusting synchronverter dynamic response speed via damping correction loop," *IEEE Transactions on Energy Conversion*, vol. 32, no. 2, pp. 608–619, 2017.

[22] S. S. Guggilam, C. Zhao, E. Dall'Anese, Y. C. Chen, and S. V. Dhople, "Optimizing DER participation in inertial and primary-frequency response," *IEEE Transactions on Power Systems*, vol. 33, no. 5, pp. 5194–5205, 2018.

[23] A. R. Al-Roomi, "Power Flow Test Systems Repository," Halifax, Nova Scotia, Canada, 2015. [Online]. Available: https://al-roomi.org/power-flow

[24] The ILOG CPLEX, 2018. [Online]. Available: http://www.ilog.com/products/cplex/

[25] F. Milano, "An open source power system analysis toolbox," *IEEE Transactions on Power Systems*, vol. 20, no. 3, pp. 1199–1206, Aug. 2005.

[26] S. V. Dhople, Y. C. Chen, A. Al-Digs, and A. D. Domínguez-García, "Reexamining the distributed slack bus," *IEEE Transactions on Power Systems*, vol. 35, no. 6, pp. 4870–4879, Nov. 2020.

[27] I. Hiskens, "Ieee pes task force on benchmark systems for stability controls," *Technical report*, 2013.